AIMS Mathematics, 11(4): 10668–10693.
DOI: 10.3934/math.2026439
Received: 01 February 2026
Revised: 04 April 2026
Accepted: 08 April 2026
Published: 20 April 2026

http://www.aimspress.com/journal/Math

Research article

Analytical investigation and in-depth analysis of the new concatenated derivative nonlinear Schrödinger equation in plasma physics

Asma AlThemairi[1] **and Rahmatullah Ibrahim Nuruddeen**[2,3,4,*]

[1] Department of Mathematical Sciences, College of Science, Princess Nourah bint Abdulrahman University, P.O. Box 84428, Riyadh 11671, Saudi Arabia

[2] Department of Mathematics, Faculty of Physical Sciences, Federal University Dutse, P.O. Box 7156, Dutse, Jigawa State, Nigeria

[3] Faculty of Education and Arts, Sohar University, Sohar 311, Oman

[4] Department of Mathematical Sciences, Saveetha School of Engineering, Saveetha Institute of Medical and Technical Science, Chennai-602105, Tamilnadu, India

* **Correspondence:** Email: rahmatullah.n@fud.edu.ng.

Abstract: Recently, Zayed et al. [4] unified the three well-known derivative nonlinear Schrödinger equations (DNLSEs) into a single concatenated DNLSE that preserves the respective properties of the individual models while introducing additional complexities and flexibilities relevant to plasma waves. This new model was thoroughly examined in the present manuscript, with a focus on unraveling some of its salient properties. The study was therefore directed toward constructing various solitonic and periodic solutions using two promising analytical methods, analyzing the resulting linearized dispersion relation, examining the possibility of modulation instability, and, lastly, analyzing the bifurcation dynamics in the posed coupled nonlinear dynamical system. In addition, based on the aforementioned analyses and appropriate numerical simulations, this study reported that the complex-valued wave profile of the new model is strongly influenced by temporal variations and by parameters arising from the adopted analytical methods. Additionally, the linearized dispersion relation has been noted to mainly disturb by the linearization parameter and the coefficient of the group-velocity dispersion. Moreover, the discovered non-singular dynamical system revealed convergent periodic and heart-like limit cycles, while firmly remaining responsive to the initial conditions change. Indeed, across the established results from the constructed soliton solutions, dispersion relation analysis, modulation instability, and bifurcation analysis, the take-home remained the attainment of optimal dispersion dynamics for plasma waves, like the Alfv́en and Langmuir waves through the unified concatenation controlling parameters, including cold-plasma environments. Finally, this study recommends further undertakings from different perspectives. In particular, one may extend the model by incorporating higher-order and perturbation terms, or extending the new

equation to a higher-dimensional form, capable of modeling several nonlinear complex physical scenarios.

Keywords: concatenation model; soliton solutions; linearized dispersion relation; modulation instability; bifurcation analysis
Mathematics Subject Classification: 35C07, 35C08, 83C15

1. Introduction

The class of derivative nonlinear Schrödinger equations (DNLSEs) is a special one in the hierarchy of complex-valued nonlinear Schrödinger equations (NLSEs) that play a vital role in the dispersion of plasma waves, including the Alfv́en and Langmuir waves, and is thus suitable for cold-plasma arenas, among others [1–3]. Certainly, studies in [1–3] gave the three most notable DNLSEs, which comprise the Kaup-Newell equation, Chen-Lee-Lie equation, and Gerjikov-Ivanov equation. These equations are known for their significant applications in the dynamics of Alfven waves, Langmuir waves, and cold plasmas, respectively, to mention a few. Moreover, for the first time, Zayed et al. [4], in 2025, unified the mentioned three complex-valued DNLSEs "along the same lines as the concatenation model and the dispersive concatenation model from optics" into a single concatenated equation that is capable of highlighting all the features of the individual equations and more, in addition to presenting of the model's integrability and solitonic analyses. This new model is the subject of the present study. The wider class of NLSEs have been much discussed the literature, and the application of these equations in various areas of modern science and technology cannot be estimated; read [5–8] for the flavor of these applications. Additionally, having unanimously referred to the solutions being satisfied by these equations as soliton or solitary waves and having fully attained certain characterizations [9–11], researchers have directed much attention into the division of effective methods for the determination of valid solitons for NLSEs and DNLSEs, including the class of resonant NLSEs [12, 13], which is essential in the study of wave phenomena in planar waveguides and optical fibers, to mention a few [14]. In this regard, several methods within analytical framework have been proposed to untangle solitonic and other solutions for NLSEs, like the modified extended direct algebraic techniques [15,16], improved modified extended tanh function method [17], and approaches that construct assorted solitons like the modified exp-function technique, general projective Riccati approach, and new generalized methods [18]. More so, other analytical methods include the extended F-expansion method [19], the modified Sardar sub-equation method [20], the expansion method [21], the dark and bright optical ansatz [22], dispersive optical solitons [23], resonant optical structures [24], the improved extended mapping technique [25], the enhanced Kudryashov approach [26], the simple equation method [27], and the $\frac{G'}{G}$-expansion methods [28].

Moreover, modeling-wise, several scientists have modified various existing complex-valued nonlinear evolution equations for various purposes. In this regard, we recall the recent studies that examined and extended NLSEs by incorporating higher-order dispersion terms, including cubic-quintic-septic-nonic nonlinearity [29, 30] and cubic-quintic-septic-nonic nonlinearity geared toward cubic-quartic NLSEs [31, 32], among others, highlighting their various applications in

nonlinear media, including the dispersion of $LiNbO_3$ crystals [26], among others. Besides, the application and incorporation of the quadratic derivative term has been stated in the good work by Das et al. [33], while the study by Broglie [34] extensively discussed the relevance of the derivative term in the evolution of resonant NLSEs. However, the current study aims to deeply examine the new unified DNLSEs [4] considering various perspectives, where the model features dissimilar complexities and flexibilities relevant to plasma waves. This model incorporates three models classical DNLSEs, having higher-order and derivative terms, which presides over the "control shape asymmetry, chirp, effective group velocity, amplitude–width trade-off, and saturation". Accordingly, the study first adopted the addendum to the Kudryashov method [35] and the modified extended tangent expansion method [8] for the construction of various solitonic and periodic solutions. In addition, the study proceeds with the analysis of the consequent linearized dispersion relation, an approach for a complete analysis of wave dynamics in solid mechanics [36, 37]. Next, the study gives a thorough examination of the modulation instability of the model, an avenue that gives the prediction and control of the undisturbed evolution of waves in the given medium [38, 39]. Moreover, the study concludes with an in-depth analysis of bifurcation dynamics of the resultant coupled nonlinear dynamical system [40, 41]. What is more, suitable fixed parameter values are searched for the numerical simulation of the results, where several findings have been noted, including the fact that the complex-valued wave profile has been observed to be influenced by temporal variation and the variation of the arising parameters from the adopted analytical methods. Next, the linearized dispersion relation has been observed to be influenced by the linearization parameter z, and the coefficient of the group-velocity dispersion a. In addition, the consequent dynamical system, when numerically simulated, reveals convergent periodic limit and heart-like limit cycles. Besides, the nonlinear system is equally noted to be sensitive to changes of the initial conditions, especially when the initial conditions are considered close to zero, due to the arisen singularity point. Certainly, these findings contribute through the attainment of optimal dispersion dynamics in plasma waves, such as Alfv́en and Langmuir waves through the unified concatenation controlling parameters, including cold-plasma environments. Finally, this manuscript is arranged in the following format: Section 2 presents the governing model and its subsequent special forms. Section 3 gives the adopted analytical procedures. Section 4 provides the analytical solutions. Section 5 analyzes the consequent linearized dispersion relation and modulation instability. Section 6 is reversed for the bifurcation analysis. Section 7 provides numerical results. Section 8 gives the conclusion of the study.

2. The new concatenated nonlinear model

Recently, Zayed et al. [4], in 2025, unified the well-known three DNLSEs into a single concatenated DNLSE that takes the following structural form:

$$\iota q_t + a q_{xx} + \iota \left(c_1 |q|^2 q_x + c_2 \left(|q|^2 q \right)_x \right) + c_3 \left(\iota b_1 q^2 q_x^* + b_2 |q|^4 q \right) = 0, \tag{2.1}$$

where $q = q(x,t)$ is the complex wave profile, while $q^* = q^*(x,t)$ is the conjugate of q, ι is the imaginary unit, such that $\iota^2 = -1$, a is the coefficient of the group-velocity dispersion, while c_1, c_2, c_3, b_1, and b_2 are all constant parameters that are non-zeros and are related to the physical scenarios, including high-order dispersion and derivative nonlinearity terms.

Moreover, the governing model in Eq (2.1) systematically reduces to the three most important complex-valued DNLSEs, including:

i). **The Kaup-Newell equation:** when $c_1 = c_3 = 0$, the new concatenated DNLSE expressed in Eq (2.1) thus reduces to the Kaup-Newell equation as follows [1]:

$$\iota q_t + a q_{xx} + \iota c_2 \left(|q|^2 q\right)_x = 0, \tag{2.2}$$

ii). **The Chen-Lee-Liu equation:** when $c_2 = c_3 = 0$, the new concatenated DNLSE expressed in Eq (2.1) thus reduces to the Chen-Lee-Liu equation as follows [2]:

$$\iota q_t + a q_{xx} + \iota c_1 |q|^2 q_x = 0, \tag{2.3}$$

iii). **The Gerjikov-Ivanov equation:** when $c_1 = c_2 = 0$, the new concatenated DNLSE expressed in Eq (2.1) thus reduces to the Gerjikov-Ivanov equation as follows [3]:

$$\iota q_t + a q_{xx} + \iota d_1 q^2 q^* + d_2 |q|^4 q = 0, \tag{2.4}$$

where $d_1 = c_3 b_1$ and $d_2 = c_3 b_2$.

Remarkably, the individual DNLSEs in Eqs (2.2)–(2.4) are used to make the concatenated DNLSE in Eq (2.1), where "the tunable derivative couplings $\{c_1, c_2, c_3\}$ and higher-order amplitudinal terms $\{b_1, b_2\}$ enable controlled passage between convective self-steepening, mixed derivative nonlinearities and quintic saturation. This structure is novel in providing a unified description that consolidates previously separate DNLS-type models into a single tractable form, thereby enabling systematic exploration of plasma nonlinearities across distinct physical regimes" [4]. In particular, "the model consolidates dynamics relevant to Langmuir waves, Alfv́en waves, and cold-plasma settings, offering one tractable formulation for disparate regimes. The derivative couplings to $\{c_1, c_2, c_3\}$ encode convective self-steepening and mixed derivative nonlinearities that arise in magnetized plasmas due to velocity-dependent phase modulation and higher-order nonlinear dispersion. The saturation terms to $\{b_1, b_2\}$ regulate strong-amplitude behavior, preventing unbounded growth and adjusting background equilibria" [4]. In addition, it is worth noting that the class of DNLSEs plays a vital role in plasma and water waves and quantum field theory, among others. The aforementioned equations have notable applications in the dynamics of Alfven and Langmuir waves, and in cold plasmas and nonlinear fiber optical arenas [1–3]. In addition, the modification and extension of nonlinear equations to incorporate higher-order dispersion and derivative terms is not new in mathematical physics and modeling. In fact, several authors coined different models in [30–32], highlighting their applications in nonlinear media. What is more, incorporation of higher-order terms, derivative terms, and resonant terms, including potential applications, is extensively discussed in the notable works of Das et al. [33] and Broglie [34], among others. Consequently, this study extensively examines the new model expressed in Eq (2.1) from different perspectives of linear and nonlinear wave dynamics.

3. Analytical methods

This section presents the chosen analytical methods for the study of the governing model. In presenting these methods, let us consider a generalized DNLSE of the following form:

$$P(q, q_t, q_x, q_{tx}, q_{tt}, q_{xx}, q_{txx}, ...) = 0. \tag{3.1}$$

Therefore, to convert the latter equation into a coupled system of real-valued nonlinear ordinary differential equations, the following complex-valued transformation is deployed:

$$q(x,t) = \psi(\xi)e^{\iota h(x,t)}, \tag{3.2}$$

where $\iota^2 = -1$ is the imaginary number, while ξ and $h(x,t)$ are transformations that read

$$\xi = x - \upsilon t \qquad \text{and} \qquad h(x,t) = -kx + \omega t, \tag{3.3}$$

where ν, k, and ω are non-zero constants, presiding over the propagation of the soliton in the examining nonlinear media. Accordingly, upon plugging Eqs (3.2) and (3.3) into Eq (3.1), one gets the resulting differential equation as follows:

$$Q(\psi(\xi), \psi'(\xi), \psi''(\xi), \psi'''(\xi), ...) = 0, \tag{3.4}$$

where the primes in the latter equation denote derivatisation, that is, $\psi'(\xi) = \frac{\mathrm{d}\psi}{\mathrm{d}\xi}, \psi''(\xi) = \frac{\mathrm{d}^2\psi}{\mathrm{d}\xi^2}$, $\psi'''(\xi) = \frac{\mathrm{d}^3\psi}{\mathrm{d}\xi^3}, ...$

3.1. Addendum to the Kudryashov method

For the application of the addendum to the Kudryashov method with order unity, Eq (3.4) admits the following series solution [35]:

$$\psi(\xi) = \sum_{j=0}^{M} f_j \phi^j(\xi), \tag{3.5}$$

where f_j for $j \geq 0$ are constants that are not all equal to zero, and the function $\phi(\xi)$ satisfies the nonlinear differential equation

$$(\phi'(\xi))^2 = \phi^2(\xi)(1 - s\phi^2(\xi)) \ln^2(r), \tag{3.6}$$

where $s \neq 0$ and $1 \neq r > 0$ are constants. Precisely, s is the addendum to the Kudryashov method parameter, while r is the logarithmic parameter. In addition, Eq (3.6) portrays the following exact solution:

$$\phi(\xi) = \frac{4\varepsilon}{s \exp_r(-\xi) + 4\varepsilon^2 \exp_r(\xi)} = \begin{cases} \frac{1}{2\varepsilon}\mathrm{csch}\left(\ln(r)\xi\right), & \text{for} \quad s = -4\varepsilon^2, \\ \\ \frac{1}{2\varepsilon}\mathrm{sech}\left(\ln(r)\xi\right), & \text{for} \quad s = 4\varepsilon^2, \end{cases} \tag{3.7}$$

where $\varepsilon(\neq 0)$ is a non-zero constant, and $\exp_r(\pm\xi) = r^{\pm\xi}$. Notably, the hyperbolic functions csch(.) and sech(.) are widely referred to as singular and bright solitons, respectively.

What is more, M appearing in the summation expressed in Eq (3.5) is a positive integer, which is plainly determined using following relationships:

$$D\left\{\psi^u(\xi)\right\} = Mu, \quad D\left\{\frac{d^v\psi}{d\xi^v}\right\} = M + v, \quad D\left\{\psi^v\left(\frac{d^u\psi}{d\xi^u}\right)^p\right\} = Mv + p(M + u), \tag{3.8}$$

where D in the latter equation denotes the degree of the bracketed expression(s).

Lastly, one substitutes Eq (3.5) into Eq (3.4), alongside Eq (3.6), to get the overall system of algebraic equations, which will be solved analytically for f_j ($j \geq 0$). Accordingly, upon getting the solution of the coupled system of algebraic equations, one gets the solution of the model expressed in Eq (3.4), which thus leads to the solution of the governing equation in Eq (3.1) through the transformation mentioned in Eqs (3.2) and (3.3).

3.2. Modified extended tangent expansion method

For the application of the modified extended tangent expansion method, Eq (3.4) admits the following series solution [8]:

$$\psi(\xi) = \sum_{j=0}^{M} f_j \phi^j(\xi) + \sum_{j=1}^{M} g_j \phi^{-j}(\xi), \tag{3.9}$$

where f_0, $f_j (j \geq 1)$, and $g_j (j \geq 1)$ are constants that are not all equal to zero, which are to be obtained later. In addition, the function $\phi(\xi)$ in Eq (3.9) satisfies the following differential equation:

$$\phi'(\xi) = \phi^2(\xi) + s, \tag{3.10}$$

where $s \neq 0$ is a non-zero real constant. Furthermore, Eq (3.10) admits exact solutions as follows:

$$\phi(\xi) = \begin{cases} -\sqrt{-s}\coth(\sqrt{-s}\xi) \text{ and } -\sqrt{-s}\tanh(\sqrt{-s}\xi), & \text{for} \quad s < 0, \\ -\sqrt{s}\cot(\sqrt{s}\xi) \text{ and } \sqrt{s}\tan(\sqrt{s}\xi), & \text{for} \quad s > 0. \end{cases} \tag{3.11}$$

What is more, M appearing in the summation expressed in Eq (3.9) is a positive integer, which is equally determined using Eq (3.8). In addition, the hyperbolic functions, coth(.) and tanh(.), are largely referred to as singular and dark soliton solutions, correspondingly.

Accordingly, upon substituting Eq (3.9) into Eq (3.4), alongside Eq (3.10), we get the overall system of algebraic equations, which will be solved analytically for f_0, f_j, and g_j $(j \geq 1)$. In the same way, upon finding the solution of the coupled system of algebraic equations, one gets the solution of Eq (3.4), which then leads to the acquisition of the solution of the governing equation in Eq (3.1) through the transformation mentioned in Eqs (3.2) and (3.3). Notably, this study exclusively makes use of *Wolfram Mathematica 9.0* for the computational and graphical illustration. The choice of the aforementioned methods [8, 35] is characterized by their simple implementations, yet they are very effective in producing assorted solitonic and periodic solutions for nonlinear evolution equations. Indeed, through the adopted methods, one constructs three classes of solutions, including exponential solutions, periodic solutions, and hyperbolic solutions, which are the widely used solutions in the open literature, featuring mainly dark, bright, and other solitons for their relevance in nonlinear optical processes.

4. Analytical investigation

With the deployment of the transformation in Eq (3.2) into Eq (2.1) of the form:

$$q(x,t) = p(\xi)e^{ih(x,t)}, \quad \xi = x - \nu t, \quad h(x,t) = -kx + \omega t, \tag{4.1}$$

one gets the resulting coupled system of nonlinear differential equations from the real and imaginary parts as follows:

$$ap''(\xi) - (\omega + ak^2)p(\xi) + k(c_1 + c_2 - c_3 b_1)p^3(\xi) + c_3 b_2 p^5(\xi) = 0 \tag{4.2}$$

and

$$-(\nu + 2ak)p'(\xi) + (c_1 + 3c_2 + c_3 b_1)p'(\xi)p^2(\xi) = 0, \tag{4.3}$$

where the last equation shows $v = -2ak$ and $c_1 + 3c_2 + c_3b_1 = 0$ for the soliton existence. Moreover, upon homogeneously balancing the real part of the model, that is, Eq (4.2), one gets $M = \frac{1}{2}$, which necessitates yet an additional transformation of the form

$$p(\xi) = \sqrt{\psi(\xi)}, \tag{4.4}$$

which subsequently yields the following nonlinear differential equation:

$$\gamma_1\psi(\xi)\psi''(\xi) + \gamma_2(\psi'(\xi))^2 + \gamma_3\psi^2(\xi) + \gamma_4\psi^3(\xi) + \gamma_5\psi^4(\xi) = 0, \tag{4.5}$$

where γ_j for $j = 1, 2, ..., 5$ are expressed as

$$\gamma_1 = \frac{a}{2}, \quad \gamma_2 = \frac{a}{4}, \quad \gamma_3 = -(\omega + ak), \quad \gamma_4 = k(c_1 + c_2 - c_3b_1), \quad \gamma_5 = c_3b_2. \tag{4.6}$$

In addition, upon homogeneously balancing Eq (4.5), one gets $M = 1$, which will be used in the subsequent subsections to construct several exact solutions for the governing new concatenated DNLSE.

4.1. Addendum to the Kudryashov method

With the determination of $M = 1$, the addendum to the Kudryashov method through Eq (3.5) gives the following solution form:

$$\psi(\xi) = f_0 + f_1\phi(\xi), \tag{4.7}$$

where f_0, and f_1, are constants that are not all equal to zero that are yet to be determined. Accordingly, upon substituting Eq (4.7) into Eq (4.5), the following system of algebraic equations is obtained:

$$\gamma_5 f_0^4 + \gamma_4 f_0^3 + \gamma_3 f_0^2 = 0, \;\; 4\gamma_5 f_1 f_0^3 + 3\gamma_4 f_1 f_0^2 + 2\gamma_3 f_1 f_0 + \gamma_1 f_1 f_0 \ln^2(r) = 0,$$

$$\gamma_3 f_1^2 + 3\gamma_4 f_0 f_1^2 + 6\gamma_5 f_0^2 f_1^2 + \gamma_1 f_1^2 \log^2(r) + \gamma_2 f_1^2 \ln^2(r) = 0,$$

$$\gamma_4 f_1^3 + 4\gamma_5 f_0 f_1^3 - 2\gamma_1 f_0 f_1 s \ln^2(r) = 0, \gamma_5 f_1^4 - 2\gamma_1 f_1^2 s \log^2(r) - \gamma_2 f_1^2 s \ln^2(r) = 0.$$

When analytically solved, we have the following solution set:

$$f_0 = -\frac{3\gamma_4}{8\gamma_5}, \;\; f_1 = \left\{-\frac{3\gamma_4\sqrt{s}}{8\gamma_5}, \frac{3\gamma_4\sqrt{s}}{8\gamma_5}\right\}, \;\; \gamma_1 = \frac{3\gamma_4^2}{32\gamma_5\ln^2(r)}, \;\; \gamma_2 = -\frac{3\gamma_4^2}{64\gamma_5\ln^2(r)}, \;\; \gamma_3 = \frac{15\gamma_4^2}{64\gamma_5}. \tag{4.8}$$

Accordingly, the adopted modified Kudryashov method reveals the following exponential solitonic solution:

$$q(x,t) = \sqrt{-\frac{3\gamma_4\left(2\varepsilon r^{(x-vt)} + \sqrt{s}\right)^2}{8\gamma_5\left(4\varepsilon^2 r^{2(x-vt)} + s\right)}}e^{\iota(-kx+\omega t)}, \tag{4.9}$$

where γ_4 and γ_5 are given in Eq (4.6), $r \neq 1$, and $s \neq 0$, such that $8\gamma_5\left(4\varepsilon^2 r^{2(x-vt)} + s\right) \neq 0$. In addition, the latter equation further disintegrates to singular and bright soliton solutions, respectively, as follows:

$$q(x,t) = \begin{cases} \sqrt{\frac{1}{2\varepsilon}\text{csch}[\ln(r)(x-vt)]}e^{\iota(-kx+\omega t)}, & s = -4\varepsilon^2, \\ \\ \sqrt{\frac{1}{2\varepsilon}\text{sech}[\ln(r)(x-vt)]}e^{\iota(-kx+\omega t)}, & s = 4\varepsilon^2. \end{cases} \tag{4.10}$$

Remarkably, the constructed solutions given above are derived with the help of an addendum to the Kudryashov method [35]. Moreover, other variants of the Kudryashov method could equally be utilized to construct assorted solutions for the model, portraying solitonic solutions like exponential solutions, hyperbolic solutions, and rational solutions, among others. Certainly, other variants of this very method that perfectly matched the current model include the classical Kudryashov method [42], the generalized Kudryashov methods [43, 44], the general improved Kudryashov method [45], and the extended generalized Kudryashov method [46]. Thus, with the adaptation of the mentioned approaches, one gets several forms of solitonic and periodic solutions.

4.2. Modified extended tangent expansion method

In the same vein, with the determination of $M = 1$, the modified extended tangent expansion method through Eq (3.9) gives the following solution form:

$$\psi(\xi) = f_0 + f_1\phi(\xi) + g_1\phi^{-1}(\xi), \tag{4.11}$$

where f_0, f_1 and g_1, are constants that are not all equal to zero. Accordingly, upon substituting Eq (4.11) into Eq (4.5), the following system of algebraic equations is obtained:

$$\gamma_5 g_1^4 + 2\gamma_1 g_1^2 s^2 + \gamma_2 g_1^2 s^2 = 0,\ 4\gamma_5 f_0 g_1^3 + 2\gamma_1 f_0 g_1 s^2 + \gamma_4 g_1^3 = 0,$$

$$4\gamma_5 f_1 g_1^3 + 3\gamma_4 f_0 g_1^2 + 6\gamma_5 f_0^2 g_1^2 + 2\gamma_1 f_1 g_1 s^2 - 2\gamma_2 f_1 g_1 s^2 + \gamma_3 g_1^2 + 2\gamma_1 g_1^2 s + 2\gamma_2 g_1^2 s = 0,$$

$$4\gamma_5 f_0^3 g_1 + 3\gamma_4 f_0^2 g_1 + 2\gamma_3 f_0 g_1 + 12\gamma_5 f_1 f_0 g_1^2 + 3\gamma_4 f_1 g_1^2 + 2\gamma_1 f_0 g_1 s = 0,$$

$$\gamma_5 f_0^4 + \gamma_4 f_0^3 + \gamma_3 f_0^2 + 12\gamma_5 f_1 f_0^2 g_1 + 6\gamma_4 f_1 f_0 g_1 + 2\gamma_3 f_1 g_1 + 6\gamma_5 f_1^2 g_1^2 + 4\gamma_1 f_1 g_1 s - 4\gamma_2 f_1 g_1 s + \gamma_2 f_1^2 s^2 + \gamma_2 g_1^2 = 0,$$

$$4\gamma_5 f_1 f_0^3 + 3\gamma_4 f_1 f_0^2 + 2\gamma_3 f_1 f_0 + 12\gamma_5 f_1^2 f_0 g_1 + 3\gamma_4 f_1^2 g_1 + 2\gamma_1 f_1 f_0 s = 0,$$

$$\gamma_3 f_1^2 + 3\gamma_4 f_0 f_1^2 + 6\gamma_5 f_0^2 f_1^2 + 4\gamma_5 f_1^3 g_1 + 2\gamma_1 f_1 g_1 - 2\gamma_2 f_1 g_1 + 2\gamma_1 f_1^2 s + 2\gamma_2 f_1^2 s = 0,$$

$$\gamma_4 f_1^3 + 4\gamma_5 f_0 f_1^3 + 2\gamma_1 f_0 f_1 = 0,\ \gamma_5 f_1^4 + 2\gamma_1 f_1^2 + \gamma_2 f_1^2 = 0.$$

Solving the above system yields several cases for hyperbolic and periodic solutions, as demonstrated in the subsequent subsections.

4.2.1. Hyperbolic solutions

Upon solving the above system, some new hyperbolic solitonic solutions are thus constructed upon considering $s < 0$ while solving the system to reveal the following solution sets:

Set 1:

$$\begin{gathered} f_1 = \{0, f_1\}, \qquad g_1 = \{g_1, 0\}, \qquad \gamma_1 = \left\{\frac{-4\gamma_5 f_0^4 - \gamma_4 f_0^3}{2g_1^2}, -\frac{f_1^2(\gamma_4 + 4\gamma_5 f_0)}{2f_0}\right\}, \\ \gamma_2 = \left\{\frac{f_0^3(\gamma_4 + 3\gamma_5 f_0)}{g_1^2}, \frac{f_1^2(\gamma_4 + 3\gamma_5 f_0)}{f_0}\right\},\ \gamma_3 = -2\left(2\gamma_5 f_0^2 + \gamma_4 f_0\right),\ s = \left\{-\frac{g_1^2}{f_0^2}, -\frac{f_0^2}{f_1^2}\right\}, \end{gathered} \tag{4.12}$$

which yield singular and dark soliton solutions, respectively, for $f_0 \neq 0$ as follows:

$$q(x,t) = \begin{cases} \sqrt{f_0\left(1 - \coth\left(\frac{g_1}{f_0}(x - \nu t)\right)\right)} e^{\iota(-kx+\omega t)}, \\ \\ \sqrt{f_0\left(1 - \tanh\left(\frac{g_1}{f_0}(x - \nu t)\right)\right)} e^{\iota(-kx+\omega t)}. \end{cases} \tag{4.13}$$

Set 2:

$$\begin{gathered} f_0 = f_0,\ f_1 = f_1,\ g_1 = \frac{f_0^2}{4f_1},\ \gamma_1 = -\frac{f_1^2\left(\gamma_4 + 4\gamma_5 f_0\right)}{2f_0}, \\ \gamma_2 = \frac{f_1^2\left(\gamma_4 + 3\gamma_5 f_0\right)}{f_0},\ \gamma_3 = -2\left(2\gamma_5 f_0^2 + \gamma_4 f_0\right), \end{gathered} \tag{4.14}$$

which yield a singular-dark combined soliton solution for $f_1 \neq 0$ as follows:

$$q(x,t) = \sqrt{f_0\left(1 - \frac{1}{2}\tanh\left(\frac{f_0}{2f_1}(x - \nu t)\right) - \frac{1}{2}\coth\left(\frac{f_0}{2f_1}(x - \nu t)\right)\right)} e^{\iota(-kx+\omega t)}. \tag{4.15}$$

Set 3:

$$\begin{gathered} f_0 = -\frac{3\gamma_4}{8\gamma_5},\ \ f_1 = \{0, f_1\},\ \ g_1 = \{g_1, 0\},\ \ \gamma_1 = \left\{-\frac{27\gamma_4^4}{2048\gamma_5^3 g_1^2}, -\frac{2}{3}\gamma_5 f_1^2\right\}, \\ \gamma_2 = \left\{\frac{27\gamma_4^4}{4096\gamma_5^3 g_1^2}, \frac{1}{3}\gamma_5 f_1^2\right\},\ \ \gamma_3 = \frac{3\gamma_4^2}{16\gamma_5},\ \ s = \left\{-\frac{64\gamma_5^2 g_1^2}{9\gamma_4^2}, -\frac{9\gamma_4^2}{64\gamma_5^2 f_1^2}\right\}, \end{gathered} \tag{4.16}$$

which yield singular and dark soliton solutions, respectively, for for $\gamma_5 \neq 0$ as follows:

$$q(x,t) = \begin{cases} \sqrt{-\frac{3\gamma_4}{8\gamma_5}\left(1 + \coth\left(\mu(x - \nu t)\right)\right)} e^{\iota(-kx+\omega t)}, \\ \\ \sqrt{-\frac{3\gamma_4}{8\gamma_5}\left(1 + \tanh\left(\mu(x - \nu t)\right)\right)} e^{\iota(-kx+\omega t)}, \end{cases} \tag{4.17}$$

where μ in the latter expressions is identified to be $\mu \in \left\{\frac{3\gamma_4}{8\gamma_5 f_1}, \frac{8\gamma_5 g_1}{3\gamma_4}\right\}$, independently, for $\gamma_5 \neq 0, f_1 \neq 0$, and $\gamma_4 \neq 0$.

Set 4:

$$f_0 = -\frac{3\gamma_4}{8\gamma_5},\ \ g_1 = \frac{9\gamma_4^2}{256\gamma_5^2 f_1},\ \ \gamma_1 = \frac{1}{3}(-2)\gamma_5 f_1^2,\ \ \gamma_2 = \frac{1}{3}\gamma_5 f_1^2,\ \ \gamma_3 = \frac{3\gamma_4^2}{16\gamma_5},\ \ s = -\frac{9\gamma_4^2}{256\gamma_5^2 f_1^2}, \tag{4.18}$$

which yield a singular-dark soliton combined solution for $\gamma_5 \neq 0$ and $f_1 \neq 0$ as follows:

$$q(x,t) = \sqrt{-\frac{3\gamma_4}{8\gamma_5}\left(1 + \frac{1}{2}\coth\left(\frac{3\gamma_4}{16\gamma_5 f_1}(x - \nu t)\right) + \frac{1}{2}\tanh\left(\frac{3\gamma_4}{16\gamma_5 f_1}(x - \nu t)\right)\right)} e^{\iota(-kx+\omega t)}. \tag{4.19}$$

4.2.2. Periodic solutions

Accordingly, upon solving the earlier stated system of nonlinear algebraic equations, periodic solutions are thus constructed upon restricting the parameter $s > 0$ while solving the system to pose the following solution sets:

Set 1:

$$f_0 = -\frac{\gamma_4}{3\gamma_5},\ \ f_1 = f_1,\ \ g_1 = \frac{\gamma_4^2}{18\gamma_5^2 f_1},\ \ \gamma_1 = -\frac{1}{2}\gamma_5 f_1^2,\ \ \gamma_2 = 0,\ \ \gamma_3 = \frac{2\gamma_4^2}{9\gamma_5},\ \ s = \frac{\gamma_4^2}{18\gamma_5^2 f_1^2}, \tag{4.20}$$

which yield a periodic cosecant solution for $\gamma_5 \neq 0$ and $f_1 \neq 0$ as follows:

$$q(x,t) = \begin{cases} \sqrt{\frac{\gamma_4}{3\gamma_5}\left(\sqrt{2}\csc\left(\frac{\sqrt{2}\gamma_4}{3\gamma_5 f_1}(x-\nu t)\right)-1\right)}e^{\iota(-kx+\omega t)}, \\ \\ \sqrt{-\frac{\gamma_4}{3\gamma_5}\left(\sqrt{2}\csc\left(\frac{\sqrt{2}\gamma_4}{3\gamma_5 f_1}(x-\nu t)\right)+1\right)}e^{\iota(-kx+\omega t)}. \end{cases} \tag{4.21}$$

Set 2:

$$f_0 = -\frac{3\gamma_4}{8\gamma_5},\ \ g_1 = \frac{9\gamma_4^2}{256\gamma_5^2 f_1},\ \ \gamma_1 = -\frac{2}{3}\gamma_5 f_1^2,\ \ \gamma_2 = \frac{1}{3}\gamma_5 f_1^2,\ \ \gamma_3 = \frac{15\gamma_4^2}{64\gamma_5},\ \ s = \frac{9\gamma_4^2}{256\gamma_5^2 f_1^2}, \tag{4.22}$$

which yield a periodic cosecant solution for $\gamma_5 \neq 0$ and $f_1 \neq 0$ as follows:

$$q(x,t) = \begin{cases} \sqrt{\frac{3\gamma_4}{8\gamma_5}\left(\csc\left(\frac{3\gamma_4}{8\gamma_5 f_1}(x-\nu t)\right)-1\right)}e^{\iota(-kx+\omega t)}, \\ \\ \sqrt{-\frac{3\gamma_4}{8\gamma_5}\left(\csc\left(\frac{3\gamma_4}{8\gamma_5 f_1}(x-\nu t)\right)+1\right)}e^{\iota(-kx+\omega t)}. \end{cases} \tag{4.23}$$

Comparatively, the original study by Zayed et al. [4] primarily deployed the applications of the sub-ordinary differential equation and the enhanced direct algebraic techniques to construct several elliptic and hyperbolic function solutions. In this regard, the adopted methods mainly construct three classes of solutions, including exponential solutions, periodic solutions, and hyperbolic solutions for the governing model. What is more, even though elliptic function solutions are more general, the solutions put forward by the present methods are the widely used solutions in the literature for the nonlinear complex-valued evolution equations, mainly the dark, bright, and singular solitons, due to their relevance in pulsification processes. In addition, the adopted Kudryashov method is a generalized method that gives various sets of solutions upon considering the general version of the method; a sort of generalization mostly found in Kudryashov-based methods [43–46], where Eq (3.6) is generalized to admit a general form for any $q \in \mathbb{N}$ as

$$(\phi'(\xi))^2 = \phi^2(\xi)(1 - s\phi^{2q}(\xi))\ln^2(r), \tag{4.24}$$

with $\phi(\xi)$ satisfying a generalized solution for any q as follows:

$$\phi(\xi) = \frac{4\varepsilon}{s\exp_r(-q\xi) + 4\varepsilon^2\exp_r(q\xi)} = \begin{cases} \left(\frac{1}{2\varepsilon}\mathrm{csch}\left(\ln(r)\xi\right)\right)^{1/q}, & \text{for} \quad s = -4\varepsilon^2, \\ \\ \left(\frac{1}{2\varepsilon}\mathrm{sech}\left(\ln(r)\xi\right)\right)^{1/q}, & \text{for} \quad s = 4\varepsilon^2. \end{cases} \tag{4.25}$$

What is more, concerning the stability of soliton solutions, we see that the acquired exact solutions are stable upon unraveling the resulting momentum factor $\mathcal{M}$ through the relation [47], where $\frac{\partial \mathcal{M}}{\partial \nu} > 0$, with ν as the soliton's velocity. Moreover, in the latter equation, a finite interval is sought, where one evaluates the integral that satisfies the mentioned condition for a stable exact solution.

5. Dispersion relation and modulation instability analyses

This section attempts to analytically determine and examine the consequent dispersion relation and the modulation instability through the resultant gain function. Accordingly, let us first consider the following solution form [38, 39]

$$q(x,t) = (\sqrt{z} + Q(x,t))e^{\iota z t}, \tag{5.1}$$

which necessitates the linearization of the governing model expressed in Eq (2.1), where z is the incident power constant, $Q(x,t)$ is the steady-state perturbed complex-valued wave field, and $\iota^2 = -1$. Thus, upon substituting Eq (5.1) into Eq (2.1), one thus obtains the following linearized Schrödinger differential equation:

$$z\left(5b_2c_3z - 1\right)Q + \iota Q_t + \iota z\left(b_1c_3 + c_1 + 3c_2\right)\left(Q_x + Q_x^*\right) + aQ_{xx} = 0, \tag{5.2}$$

where $Q^* = Q^*(x,t)$ is the conjugation of $Q = Q(x,t)$.

5.1. Dispersion relation analysis

Now, for the acquisition of the consequent dispersion relation, the deduced linearized Schrödinger equation in Eq (5.2) is thus solved using the following traveling harmonic wave solution:

$$\begin{aligned} Q(x,t) &= A_1 e^{\iota(Kx-\Omega t)} + B_1 e^{-\iota(Kx-\Omega t)}, \\ Q^*(x,t) &= A_1 e^{-\iota(Kx-\Omega t)} + B_1 e^{\iota(Kx-\Omega t)}, \end{aligned} \tag{5.3}$$

where Ω is the frequency, K is the wavenumber, and A_j, B_j for $j = 1, 2$, are constants to be determined. Next, upon plugging the latter solution into Eq (5.2), one gets the following coupled system of algebraic equations:

$$\mathbf{AX} = \mathbf{0}, \tag{5.4}$$

where the matrices $\mathbf{A}, \mathbf{X}$, and $\mathbf{0}$ are exclusively expressed as follows:

$$\mathbf{A} = \begin{pmatrix} a_{11} & a_{12} \\ a_{21} & a_{22} \end{pmatrix}, \quad \mathbf{X} = \begin{pmatrix} A_1 \\ B_1 \end{pmatrix}, \quad \mathbf{0} = \begin{pmatrix} 0 \\ 0 \end{pmatrix}, \tag{5.5}$$

where the entries a_{ij}, for $i, j = 1, 2$, are plainly expressed as follows:

$$\begin{aligned} &a_{11} = -aK^2 - zc_1K - 3zc_2K - zb_1c_3K - z + \Omega + 5z^2b_2c_3, \;\; a_{12} = -Kzc_1 - 3Kzc_2 - Kzb_1c_3, \\ &a_{21} = Kzc_1 + 3Kzc_2 + Kzb_1c_3, \;\; a_{22} = -aK^2 + zc_1K + 3zc_2K + zb_1c_3K - z - \Omega + 5z^2b_2c_3. \end{aligned} \tag{5.6}$$

Consequently, the consequential dispersion relation is thus determined, after equating the resultant determinant of the coefficient matrix in Eq (5.4) to zero as follows:

$$K^4 + \beta_1K^2 + \beta_2K\Omega + \beta_3\Omega^2 + \beta_4 = 0, \tag{5.7}$$

where

$$\beta_1 = \frac{2z}{a}\left(1 - 5b_2c_3z\right), \quad \beta_2 = \frac{2z}{a^2}\left(b_1c_3 + c_1 + 3c_2\right), \quad \beta_3 = -\frac{1}{a^2}, \quad \beta_4 = \frac{z^2}{a^2}\left(1 - 5b_2c_3z\right)^2. \tag{5.8}$$

Moreover, one gets the cut-off frequencies upon setting the wavenumber to zero, that is, $K = 0$ in Eq (5.7) as follows:

$$\Omega^2 - \frac{\beta_4}{\beta_3} = 0, \tag{5.9}$$

which are explicitly obtained as $\Omega = \pm\sqrt{\frac{\beta_4}{\beta_3}}$. In addition, the static equation is obtained when $\Omega = 0$ in Eq (5.7) as follows:

$$K^4 + \beta_1 K^2 + \beta_4 = 0, \tag{5.10}$$

where the roots of the static equation are explicitly determined as $K = \pm\frac{1}{\sqrt{2}}\sqrt{-\beta_1 \pm \sqrt{\beta_1^2 - 4\beta_4}}$.

5.2. Modulation instability analysis

For the analysis of the possible modulation instability, the acquired dispersion relation in Eq (5.7) is revisited by making the frequency Ω subject to the following equation:

$$\Omega = \frac{\beta_2 K \pm \sqrt{\beta_2^2K^2 + 4\beta_3\left(\beta_4 + K^4 + \beta_1K^2\right)}}{2\beta_3}. \tag{5.11}$$

Besides, with the acquisition of the explicit expression for the frequency above, one can easily determine the consequent phase (V^{ph}) and group (V^{g}) velocities, respectively, using the following formulae:

$$V^{\mathrm{ph}} = \frac{\Omega}{K} \qquad \text{and} \qquad V^{\mathrm{g}} = \frac{\mathrm{d}\Omega}{\mathrm{d}K}. \tag{5.12}$$

Furthermore, from the obtained expression for the frequency in Eq (5.11), one sees that modulation instability exists upon satisfaction of the following inequality,

$$\beta_2^2K^2 + 4\beta_3\left(\beta_4 + K^4 + \beta_1K^2\right) < 0. \tag{5.13}$$

Notably, one obtains the subsequent gain function $G(K)$ from Eq (5.11) as follows:

$$G(K) = 2\Im\left\{\frac{\beta_2 K \pm \sqrt{\beta_2^2K^2 + 4\beta_3\left(\beta_4 + K^4 + \beta_1K^2\right)}}{2\beta_3}\right\}, \tag{5.14}$$

where $\Im$ denotes the imaginary part of the enclosed expression. This function is deeply attached to the constraining condition in Eq (5.13), which ensures the modulation instability exists [38,39]. Moreover, one is referred to the recent studies in [48,49] for modern perspectives of modulation capabilities that cut across the analysis and design of modulators, sensors, and optical switches, among others, in waveguides.

6. Bifurcation analysis

First, let us re-write Eq (4.5) as follows:

$$\psi''(\xi) - D_1(\psi'(\xi))^2\psi^{-1}(\xi) - D_2\psi(\xi) + D_3\psi^2(\xi) + D_4\psi^3(\xi) = 0, \tag{6.1}$$

where

$$D_1 = \frac{1}{2}, \quad D_2 = \frac{2}{a}(\omega + ak^2), \quad D_3 = \frac{2k}{a}(c_1 + c_2 - c_3b_1), \quad D_4 = \frac{2}{a}c_3b_2. \tag{6.2}$$

Therefore, through the use of suitable Galilean transformations of the form [40, 41]

$$Y_1 = \psi(\xi) \quad \text{and} \quad Y_2 = \psi'(\xi), \tag{6.3}$$

the second-order singular nonlinear differential equation expressed in Eq (6.1) thus transforms to a coupled system of singular nonlinear first-order dynamical equations of the following form:

$$\begin{aligned} Y_1' &= Y_2, \\ Y_2' &= D_1Y_2^2Y_1^{-1} + D_2Y_1 - D_3Y_1^2 - D_4Y_1^3. \end{aligned} \tag{6.4}$$

In addition, the expected equilibrium points could be obtained from Eq (6.4) upon equating the system to zero more explicitly as follows

$$Y_1 = 0, \;\; Y_1 = w_1 \;\; \text{or} \;\; Y_1 = w_2, \;\; Y_2 = 0, \tag{6.5}$$

where w_1 and w_2 in the latter equation are plainly obtained as follows:

$$w_1 = \frac{-D_3 + \sqrt{D_3^2 + 4D_2D_4}}{2D_4} \;\; \text{and} \;\; w_2 = \frac{-D_3 - \sqrt{D_3^2 + 4D_2D_4}}{2D_4}. \tag{6.6}$$

Evidently, three equilibrium points are deduced from Eq (6.5) as follows:

$$E_0 = (0, 0), \qquad E_1 = (w_1, 0), \qquad E_2 = (w_2, 0). \tag{6.7}$$

Moreover, the coefficient matrix of the dynamical system in Eq (6.4) yields the resultant Jacobian determinant as follows:

$$\begin{aligned} J(Y_1, Y_2) &= \begin{vmatrix} 0 & 1 \\ -D_1Y_2^2Y_1^{-2} + D_2 - 2D_3Y_1 - 3D_4Y_1^2 & 2D_1Y_2Y_1^{-1} \end{vmatrix}, \\ &= D_1Y_2^2Y_1^{-2} + 2D_3Y_1 + 3D_4Y_1^2 - D_2. \end{aligned} \tag{6.8}$$

Furthermore, concerning the stability of equilibrium points, the following cases are examined in relation to the determined Jacobian determinant in Eq (6.8) concerning the established equilibrium points E_0, E_1, and E_2:

I). **Case 1:** The acquired Jacobian determinant in Eq (6.8) takes the folowing expression at E_0 :

$$\det(J)|_{E_0} = -D_2, \tag{6.9}$$

which poses the following scenarios:

i) **A saddle point** when $\det(J)|_{E_0} < 0$: with the consideration of $D_2 > 0$;
ii) **A center point** when $\det(J)|_{E_0} > 0$: with the consideration of $D_2 < 0$;
iii) **A cuspidial point** when $\det(J)|_{E_0} = 0$: with the consideration of $D_2 = 0$.

II). **Case 2:** The acquired Jacobian determinant in Eq (6.8) takes the folowing expression at E_1 :

$$\det(J)|_{E_1} = 2D_3w_1 + 3D_4w_1^2 - D_2, \tag{6.10}$$

which poses the following scenarios:

i) **A saddle point** when $\det(J)|_{E_1} < 0$: with the consideration of $D_2 > 2D_3w_1 + 3D_4w_1^2$;
ii) **A center point** when $\det(J)|_{E_1} > 0$: with the consideration of $D_2 < 2D_3w_1 + 3D_4w_1^2$;
iii) **A cuspidial point** when $\det(J)|_{E_1} = 0$: with the consideration of $D_2 = 2D_3w_1 + 3D_4w_1^2$.

III). **Case 3:** The acquired Jacobian determinant in Eq (6.8) takes the folowing expression at E_2 :

$$\det(J)|_{E_2} = 2D_3w_2 + 3D_4w_2^2 - D_2, \tag{6.11}$$

which poses the following scenarios:

i) **A saddle point** when $\det(J)|_{E_2} < 0$: with the consideration of $D_2 > 2D_3w_2 + 3D_4w_2^2$;
ii) **A center point** when $\det(J)|_{E_2} > 0$: with the consideration of $D_2 < 2D_3w_2 + 3D_4w_2^2$;
iii) **A cuspidial point** when $\det(J)|_{E_2} = 0$: with the consideration of $D_2 = 2D_3w_2 + 3D_4w_2^2$.

Remarkably, upon substituting the expressions for w_1 and w_2, earlier expressed in Eq (6.6), the latter Cases 2 and 3 could be scrutinized deeply for several other realistic scenarios. Furthermore, for an advanced-level analysis of the stability of equilibrium points, one may equally opt for the acquisition of the explicit expressions of the consequent eigenvalues of the almost linear system from Eq (6.4) through the established equilibrium points in Eq (6.7). Accordingly, one characterizes the stability of equilibrium points upon studying the complete eigenvalue characterizations, where nodal and source points are attained, including the degenerate case upon the discovery of zero characteristic value [40].

7. Numerical results and discussion

This section numerically examines some of the constructed solitonic solutions, mainly the bright and dark soliton solutions, in favor of their vast relevance in nonlinear media. In addition, the acquired linearized dispersion relation will be examined to study the impact of the involved parameters. What is more, the obtained dynamical system for the governing new model will equally be examined numerically with the application of the built-in *Wolfram Mathematica 9.0* command for the numerical solution of differential equations. Moreover, all the involved parameters are considered to be unity in the numerical simulation, unless otherwise stated. The study mainly makes use of the two-dimensional (2D) and three-dimensional (3D) plots to portray the graphical results. Notably, in contrast, it is pertinent to mention here that the original study by Zayed et al. [4] only proposed the model and presented solitonic solutions using two analytical methods, without resorting to an in-depth analysis of the model. In this regard, for the first time, this study unearthed several salient characteristics of the model through a culmination of thorough examinations, which cut across solitonic analysis, analysis of the linearized dispersion relation, examination of modulation instability,

and, lastly, the analysis of bifurcation dynamics. These examinations are portrayed graphically in what follows.

7.1. Analysis of the bright and dark soliton solution

Having constructed several solitonic and periodic solutions, this subsection thus analyses some of the acquired solutions, including the bright soliton determined in Eq (4.10) and the dark soliton determined in Eq (4.13), in favour of their vast relevance in nonlinear media. Accordingly, Figures 1–3 numerically analyse the bright soliton solution Eq (4.10) through the examination of the impact of temporal variation t, the addendum to the Kudryashov parameter ε, and the logarithmic parameter r, respectively. More precisely, Figure 1(a) analyses the bright soliton solution Eq (4.10) by studying the impact of temporal variation on the complex-valued wave profile. Notably, one observes that the wave positively progresses with an increase in time. In addition, one observes a symmetry at $x = 0$ when $t = 0$, that is, when the system is at rest. Certainly, the static behaviour captured in Figure 1(a) at $t = 0$ affirms the action of the corresponding initial condition from Eq (4.10), where the acquired complex-valued wave field is static; the fact that bright functions are even functions (another evidence for a symmetrical profile at $t = 0$). Equally, see Figure 1(b) for the pictorial view of the 3D profile of the solution. Further, Figure 2(a) analyses the impact of varying the addendum to the Kudryashov parameter ε. Indeed, one notes from the figure that increasing the addendum to the Kudryashov parameter decreases the wave's amplitude. What is more, it is clear that the wave's energy reduces with an increase in the parameter. This could be used to control the wave's dynamics in the nonlinear medium; see also Figure 2(b) for the pictorial view of the 3D profile of the solution. Furthermore, Figure 3(c) analyses the impact of varying the logarithmic parameter r, where one observes that increasing the parameter reduces the wave profile, at the same time maintaining the propagating amplitude; see Figure 3(b) for the pictorial view of the 3D profile of the solution.

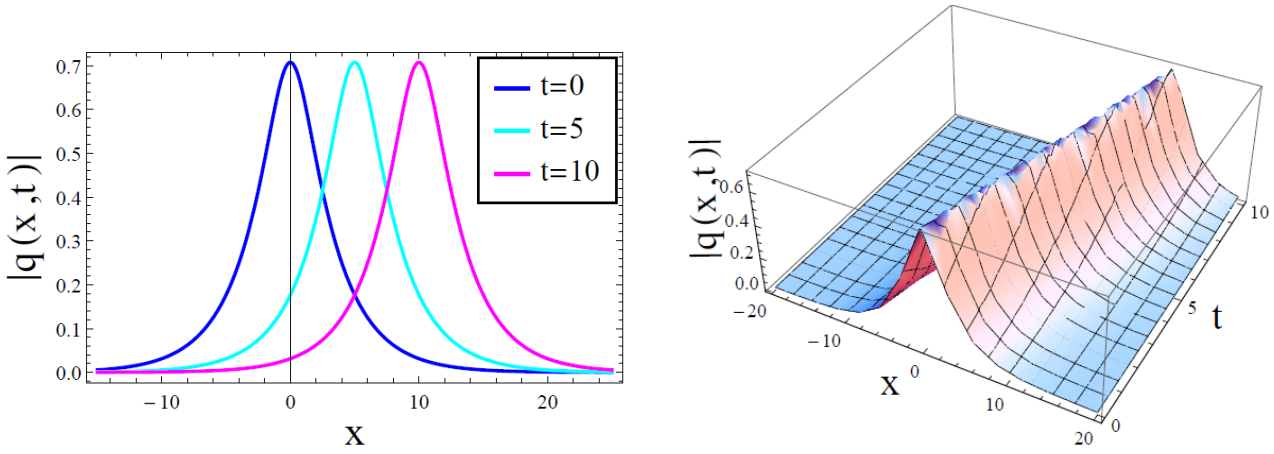

(a) 2D plot showing the effect of time variation t **(b)** 3D plot for bright soliton Eq (4.10)

Figure 1. Graphical illustrations showing the effect of temporal variation t on the bright soliton determined in Eq (4.10) when $r = 2$.

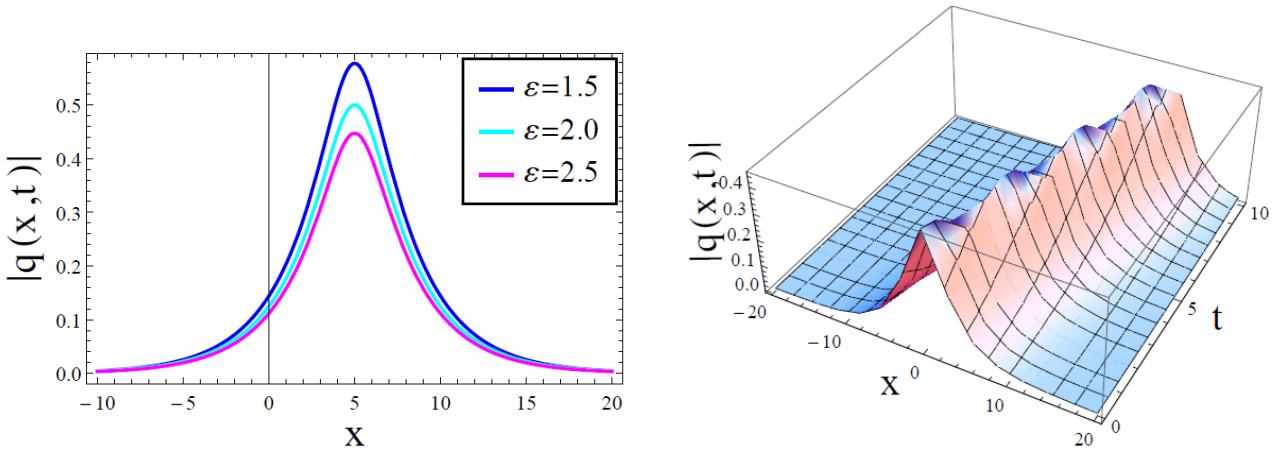

(a) 2D plot showing the effect of ε variation at $t = 5$ **(b)** 3D plot for soliton Eq (4.10) at $\varepsilon = 2.5$

Figure 2. Graphical illustrations showing the effect of the addendum to Kudryashov parameter ε on the bright soliton determined in Eq (4.10) when $r = 2$.

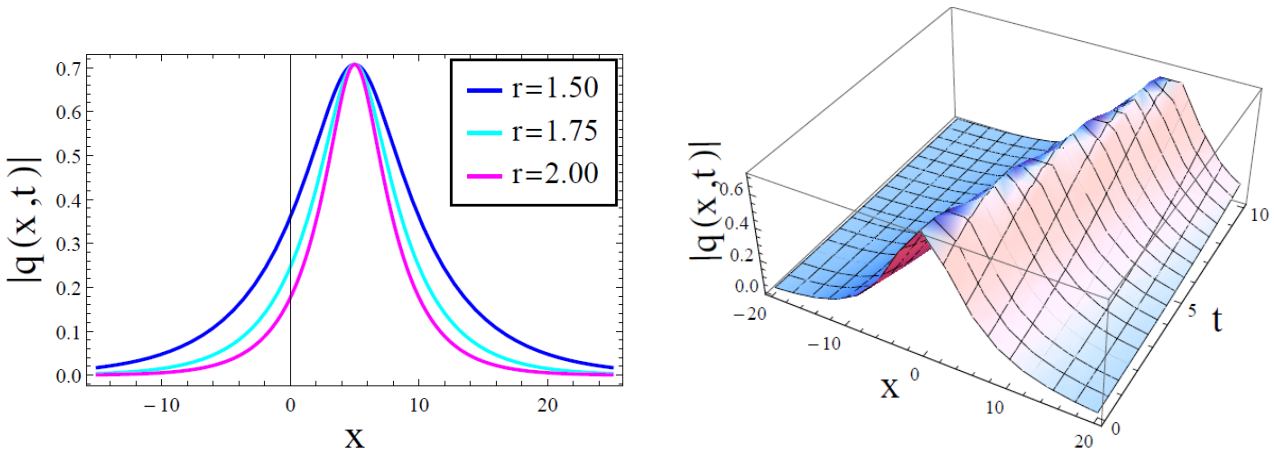

(a) 2D plot showing the effect of r variation at $t = 5$ **(b)** 3D plot for soliton Eq (4.10) at $r = 1.5$

Figure 3. Graphical illustrations showing the effect of the logarithmic parameter r on the bright soliton determined in Eq (4.10).

Figures 4 and 5 numerically analyze the dark soliton solution Eq (4.13) through the examination of the impact of temporal variation t, and that of the arising constant parameter f_0, respectively. In particular, one notes from Figure 4(a) that the wave positively progresses with an increase in time. This is already the expected trend since the solution is positive, affirming the established results in the case of a bright soliton solution; see also Figure 4(b) for the 3D depiction of the solution. Additionally, Figure 6 examines the response of the dark soliton solution Eq (4.13) to the arisen parameter f_0, where one notes that increasing the parameter increases the wave's complex-valued profile. In addition, the wave sharpens as the parameter increases; see also Figure 4(b) for the 3D depiction of the solution at $f_0 = 3$.

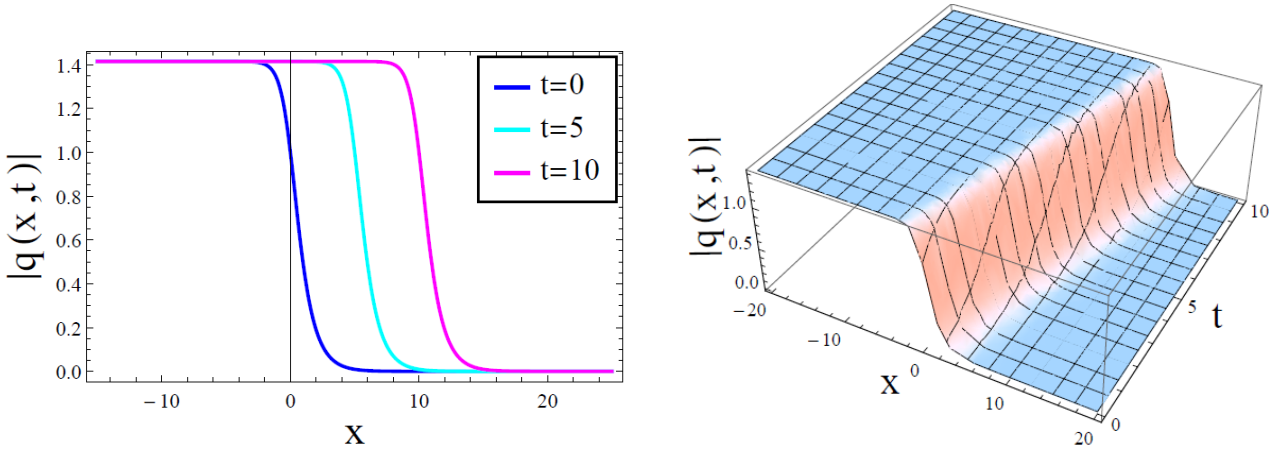

(a) 2D plot showing the effect of time variation t **(b)** 3D plot for bright soliton Eq (4.10)

Figure 4. Graphical illustrations showing the effect of the temporal variation t on the dark soliton determined in Eq (4.13).

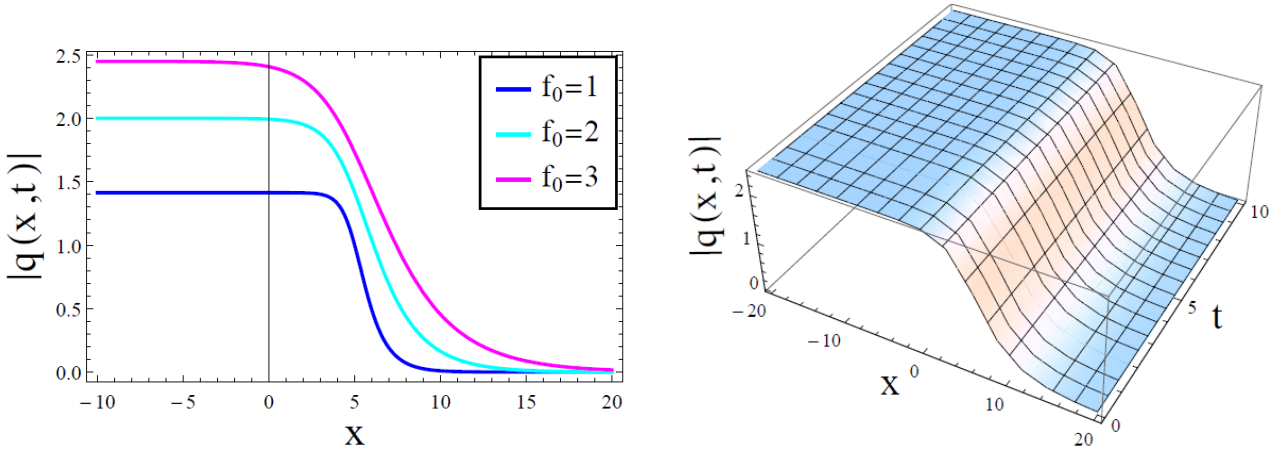

(a) 2D plot showing the effect of the f_0 at $t = 5$ **(b)** 3D plot for soliton Eq (4.13) at $f_0 = 3$

Figure 5. Graphical illustrations showing the effect of the constant parameter f_0 on the dark soliton determined in Eq (4.13).

7.2. Analysis of the linearized dispersion relation

Here, we numerically analyze the obtained linearized dispersion relation determined in Eq (5.7) via the already stated data. In particular, Figures 6 and 7, respectively, analyze the impact of varying the incident parameter z, and that of the coefficient of the group-velocity dispersion a on the dispersion of waves in the nonlinear media. 2D plots are plotted for the phase speed $\left(\frac{\Omega}{K}\right)$ against the wavenumber K. Moreover, the governing new concatenated DNLSE reduces to several models, including: the Kaup-Newell (KN) equation when $c_1 = c_3 = 0$, the Chen-Lee-Liu (CLL) equation when $c_2 = c_3 = 0$, and the Gerjikov-Ivanov (GI) equation when $c_1 = c_2 = 0$. In particular, Figure 6 shows the impact of varying the incident parameter z on the dispersion of linearized waves in the governing medium. More precisely, from Figure 6(a), one notes that increasing the incident parameter z increases the phase speed in the medium. Additionally, while the same trend has been captured in Figure 6(b) for the

special models, the CLL equation has been noted to be less responsive to the increase in z. At the same time, the GI equation has been noted to be more responsive among the three special equations.

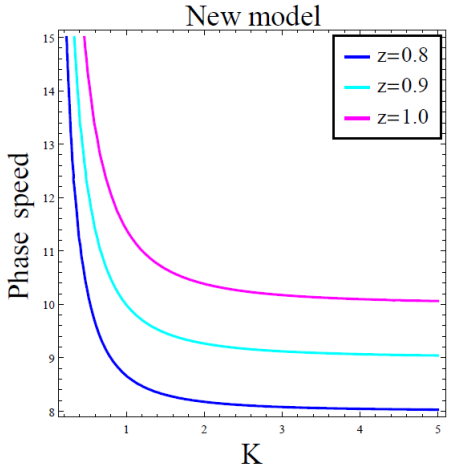

(a) Dispersion curves in the new model responding to incident power z

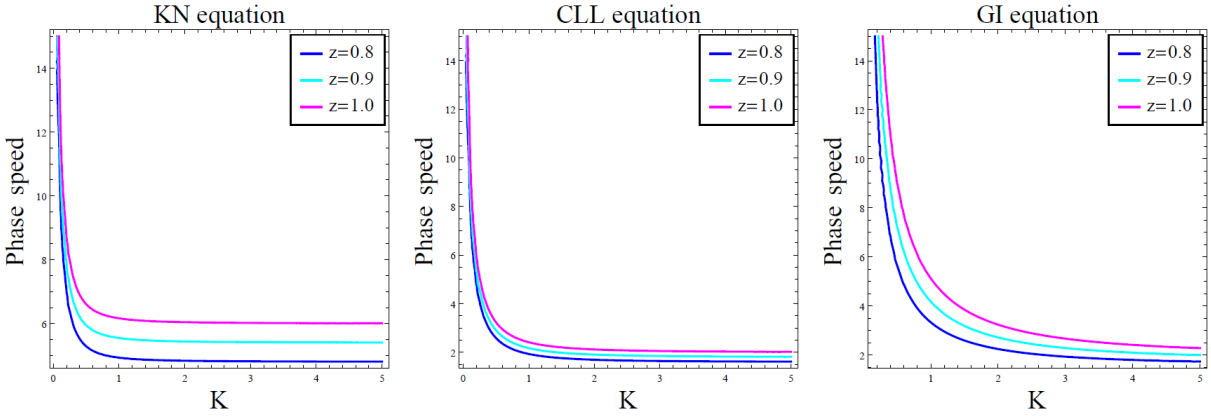

(b) Dispersion curves in the KN, CLL, and GI models responding to the incident power z

Figure 6. Dispersion curves across of the models responding to the incident power z when $a = 0.001$.

The next important parameter in the linearized dispersion relation is the coefficient of the group-velocity dispersion a, which governs the linearized dispersion in the medium, where other dispersion terms are of higher order. Thus, from Figure 7, the impact of varying a on the dispersion of waves has been captured in the medium. Precisely, one notes from Figure 7(a) that increasing the coefficient a decreases the phase speed in the medium as the wavenumber K increases. In addition, only the case of the GI equation from Figure 7(b) has been noted to equally follow the trend of Figure 7(a) for the new model; this is, however, the fact that GI equation is much closer to the new concatenated DNLSE model in terms of high-order dispersion terms in comparison to the KN and CLL equations that mainly admit a single purely derivative term. Moreover, the impact of increasing the coefficient a in the cases of the KN and CLL equations has been observed to increase the dependency of the phase speed on the wavenumber.

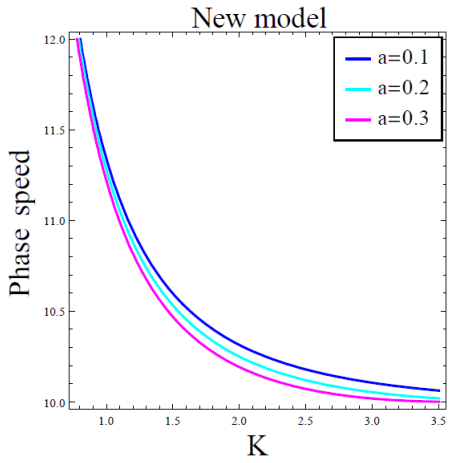

(a) Dispersion curves in the new model responding to the coefficient of group-velocity dispersion a

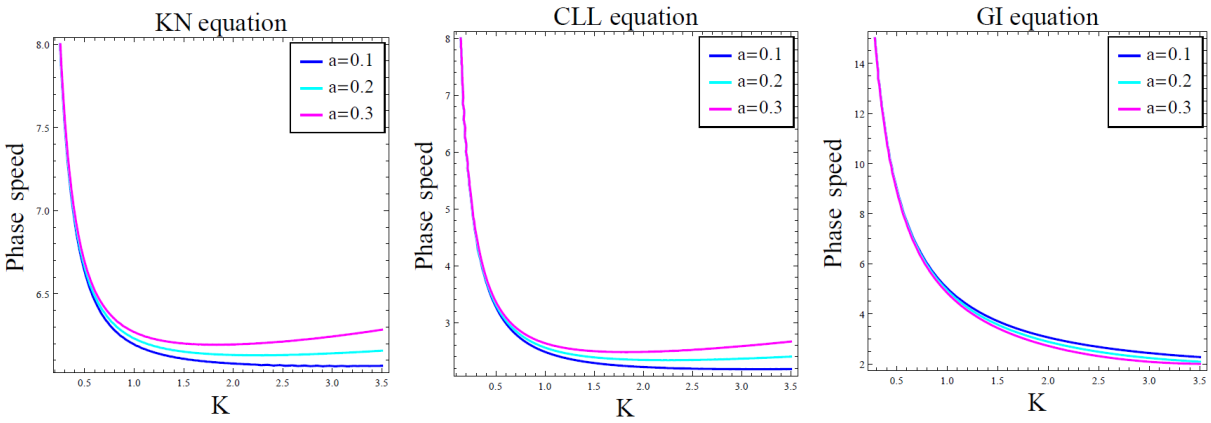

(b) Dispersion curves in the KN, CLL, and GI models responding to the coefficient of group-velocity dispersion a

Figure 7. Dispersion curves across of the models responding to the coefficient of group-velocity dispersion a.

7.3. Analysis of the dynamical system

Here, we supply the bifurcation diagrams to infer, from the discovered dynamical system in Eq (6.4), how the system evolves over ξ, as well as the wave transformation variation for the spatial and temporal variables, that is, $\xi = x - vt$. Accordingly, with the consideration of the previously mentioned fixed parameter values, Figures 8 and 9 are provided to report the evolution of the system. Indeed, from these figures, phase portraits are provided to showcase the relationships between $Y_1(\xi)$ and $Y_2(\xi)$ in Figure 8 (a) and Figure 9 (a), the relationships between $Y_1(\xi)$ and $Y_1'(\xi)$ in Figure 8 (c) and Figure 9 (c), the relationships between $Y_2(\xi)$ and $Y_2'(\xi)$ in Figure 8 (d) and Figure 9 (d), while Figure 8 (b) and Figure 9 (b) show the wave profiles for $Y_1(\xi)$ and $Y_2(\xi)$ against ξ. In particular, upon considering the initial condition in Figure 8 to be $Y_1(0) = 0.25$, and $Y_2(0) = 0.5$, one observes from the phase portraits given in Figure 8 (a), and (c) that both relationships appear to converge to periodic limit cycles, while the relationship in Figure 8 (d) appears to converge to a heart-like limit cycle.

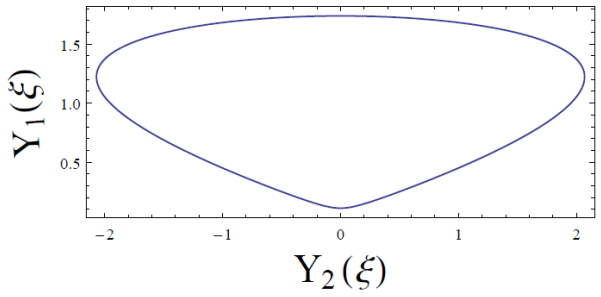

(a) Phase portrait for the relationship of Y_1 and Y_2

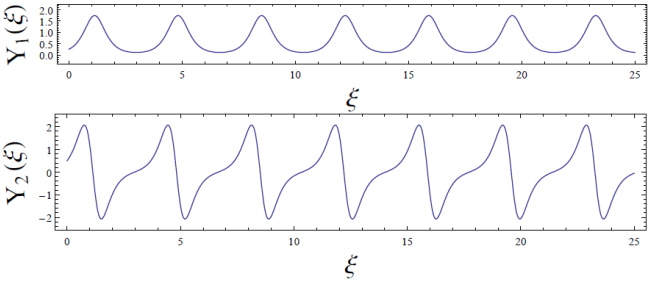

(b) Wave profiles for Y_1 and Y_2 against ξ

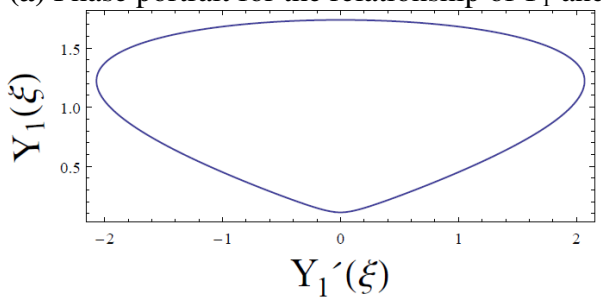

(c) Phase portrait for the relationship of Y_1 and Y_1'

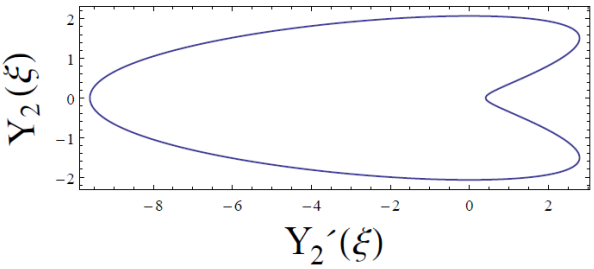

(d) Phase portrait for the relationship of Y_2 and Y_2'

Figure 8. Phase portrait showing the relationship between: (a) $Y_1(\xi)$ and $Y_2(\xi)$, (c) $Y_1(\xi)$ and $Y_1'(\xi)$, (d) $Y_2(\xi)$ and $Y_2'(\xi)$, while (b) shows the wave profiles for $Y_1(\xi)$ and $Y_2(\xi)$ against ξ when $Y_1(0) = 0.25$ and $Y_2(0) = 0.5$.

Moreover, with the reduction of the initial conditions to $Y_1(0) = 0.001$, and $Y_2(0) = 0$. Recall that the dynamical system is non-singular in Y_1; the patterns obtained in Figure 9 eventually follow the same trend with those reported in Figure 8 (a)–(c). However, the effect of a change in the initial conditions is vividly captured in bifurcation diagrams in Figures 8 (b) and 9 (b), where the latter figure has been noted to be much more stretched with longer wavelengths while affirming the earlier amplitude. In essence, the trajectory in the (Y_1, Y_2) phase plane exhibits a closed orbit, indicating the existence of periodic solutions. This suggests that the system operates in a stable oscillatory regime. The absence of spiraling trajectories or divergence implies that the system is not dissipative in the considered parameter regime, and energy-like quantities are effectively conserved. Similarly, the phase portrait in the (Y_1, Y_1') plane confirms this periodic nature, showing smooth closed curves characteristic of nonlinear oscillators. However, these curves deviate from simple ellipses, highlighting the influence of nonlinear terms. In contrast, the (Y_2, Y_2') phase portrait displays noticeable asymmetry and deformation. This behavior is primarily due to the higher-order nonlinear terms $(-D_3 Y_1^2)$ and $(-D_4 Y_1^3)$, which introduce anharmonic effects and distort the phase trajectories. In the same direction, since non-chaotic patterns are noted in the portrayed figures, more hope is then attached to numerical simulation investigation, where chaotic patterns will be attained upon experimenting with the imposed initial data. For brevity, we will leave this for another time. What is more, one then relates the bifurcation study to the earlier transformed nonlinear partial differential equation in Eq (4.2), which thus leads to the governing complex-valued DNLSE in Eq (2.1). In fact, the wave profiles $(Y_1(\xi))$ and $(Y_2(\xi))$ reveal periodic wave structures (Figures 8(b) and 9(b)). The waveform associated with (Y_1) appears nearly regular, while (Y_2) exhibits sharper gradients and

asymmetry. This difference reflects the nonlinear coupling between the variables and indicates that the system supports nonlinear periodic waves rather than purely harmonic oscillations. Such waveforms are typical in nonlinear dispersive media, where waveform distortion arises due to the balance between nonlinear steepening and dispersive spreading. Overall, the system provides a representative model for studying nonlinear wave propagation and the emergence of structured oscillatory regimes.

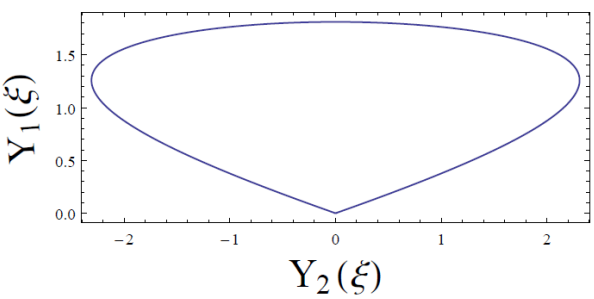

(a) Phase portrait for the relationship of Y_1 and Y_2

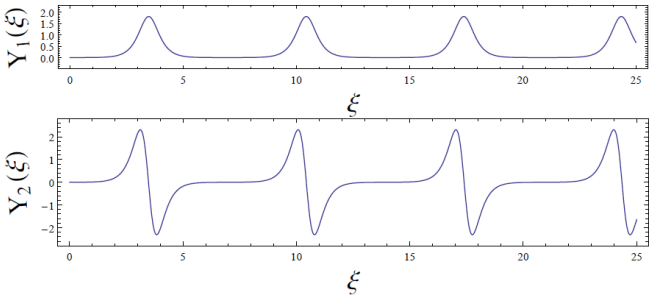

(b) Wave profiles for Y_1 and Y_2 against ξ

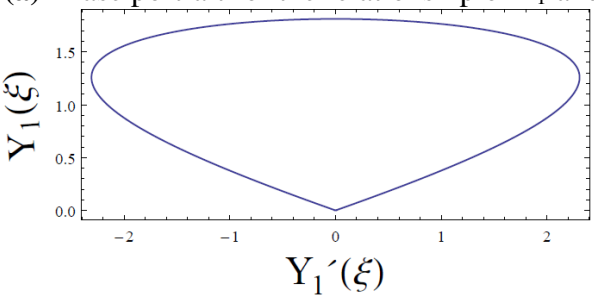

(c) Phase portrait for the relationship of Y_1 and Y_1'

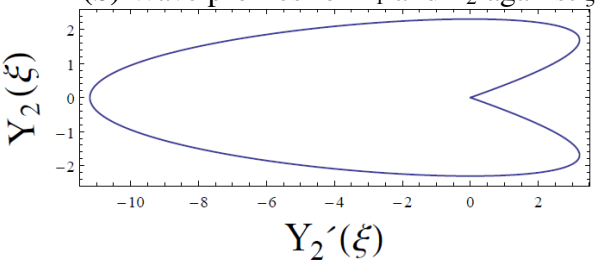

(d) Phase portrait for the relationship of Y_2 and Y_2'

Figure 9. Phase portrait showing the relationship between: (a) $Y_1(\xi)$ and $Y_2(\xi)$, (c) $Y_1(\xi)$ and $Y_1'(\xi)$, (d) $Y_2(\xi)$ and $Y_2'(\xi)$, while (b) shows the wave profiles for $Y_1(\xi)$ and $Y_2(\xi)$ against ξ when $Y_1(0) = 0.001$ and $Y_2(0) = 0$.

8. Conclusions

In conclusion, the present study deeply analyzed the recently unified DNLSE that concatenated the three most important DNLSEs: the KN, CLL, and GI equations. A deep analysis of the model was completed, which comprised constructing various solitonic and periodic solutions, linearized dispersion relation analysis, modulation instability analysis, and bifurcation analysis. Moreover, two promising analytical methods were adopted in revealing the said solutions, which vividly augmented the previously deployed variant methods, including the sub-ODE method and the direct algebraic method. Besides, the basis of solitonic analysis lies in transforming the governing model to its corresponding ODE through Lie's influenced wave transformation, while the dispersion relation and modulation instability analyses are rooted in the adaptation of harmonic-type solutions, after linearizing the nonlinear model. The bifurcation analysis equally required a transformation of the governing model to a system of first-order ODEs. Numerically, the complex-valued wave profile was noted to be much influenced by temporal variation, Kudryashov method indices, and the arising parameters from the secondary adopted method. In addition, the linearized dispersion relation was

noted to be mainly disturbed by the involved incident power and the coefficient of the group-velocity dispersion. As a special case of much interest, this analysis was extended to the KN, CLL, and GI equations. Furthermore, the derived non-singular dynamical system was numerically examined, revealing phase portraits that converged to periodic limit cycles, and a heart-like limit cycle for a particular scenario. Moreover, the dynamical system was noted to be much more responsive to the change of initial conditions; intuitively, due to the non-singularity, with bifurcation diagrams stretched with longer wavelengths when imposing initial conditions $\mathbf{Y}_j(0) << 1$, for $j = 1, 2$. The analysis demonstrates that the system exhibits stable periodic behavior characterized by closed phase trajectories and nonlinear waveforms. The interplay between linear and nonlinear terms governs the qualitative features of the dynamics. Furthermore, parameter variations are expected to induce bifurcations, leading to richer dynamical behaviors. Lastly, this study can be extended to other families of complex-valued nonlinear evolution equations arising in other fields of much concern, including optics and plasma physics, fluid dynamics, quantum mechanics, and contemporary electro-optical communications, to name a few. In particular, one may extend this new model to feature perturbation terms and dissimilar refractive index laws, thereby creating room for the effect of high-order dispersion terms, where the application of some sophisticated analytical methods will be highly required. In addition, the findings in this study will lay a solid step for the complete characterization of optimal dispersion dynamics in plasmas, where plasma waves such as Alfv́en and Langmuir waves are controlled through the new embedded parameters of tunable derivative couplings $\{c_1, c_2, c_3\}$ and higher-order amplitudinal terms $\{b_1, b_2\}$ for convective self-steepening, mixed derivative nonlinearities, and quintic saturation of the new model, which are of paramount importance in cold-plasma environments.

Author contributions

Conceptualization, AA and RIN; Methodology, AA and RIN; Software, RIN; Validation, AA and RIN; Formal analysis, AA and RIN; Investigation, AA and RIN; Resources, AA; Data curation, AA and RIN; Writing – original draft, RIN; Writing – review and editing, AA and RIN; Visualization, RIN; Supervision, AA and RIN; Project administration, AA; Funding acquisition, AA.

Use of Generative-AI tools declaration

The authors declare they have not used Artificial Intelligence (AI) tools in the creation of this article.

Acknowledgments

This work was supported by the Princess Nourah bint Abdulrahman University Researchers Supporting Project number (PNURSP2026R295), Princess Nourah bint Abdulrahman University, Riyadh, Saudi Arabia.

Funding

This research was funded by the Researchers Supporting Project number (PNURSP2026R295), Princess Nourah bint Abdulrahman University, Riyadh, Saudi Arabia.

Conflict of interest

The authors declare they have no conflict of interest.

References

1. D.J. Kaup, A. C. Newell, An exact solution for a derivative nonlinear Schroodinger equation, *J. Math. Phys.*, **19** (1978), 798–801. https://doi.org/10.1063/1.523737
2. H. H. Chen, Y. C. Lee, C. S. Liu, Integrability of nonlinear hamiltonian systems by inverse scattering method, *Phys. Scr.*, **20** (1979), 490–492. https://doi.org/10.1088/0031-8949/20/3-4/026
3. V. S. Gerdjikov, M. I. Ivanov, The quadratic bundle of general form and the nonlinear evolution equations, *Bulg. J. Phys.*, **10** (1983), 130.
4. E. M. E. Zayed, M. El–Shater, A. H. Arnous, A. Biswas, A unified concatenation model for plasma physics: Integrability and soliton solutions, *MethodsX*, **15** (2025), 103641. https://doi.org/10.1016/j.mex.2025.103641
5. K. K. Ahmed, N. M. Badra, H. M. Ahmed, W. B. Rabie, Soliton solutions of generalized Kundu-Eckhaus equation with an extra-dispersion via improved modified extended tanh-function technique, *Opt. Quant. Electron.*, **55** (2023), 299. https://doi.org/10.1007/s11082-023-04599-x
6. K. L. Wang, Diversity of soliton solutions to the nonlinear fractional Kadoma equation, *Fractals*, **34** (2025), 2550107. https://doi.org/10.1142/S0218348X25501075
7. M. N. Alshehri, S. Althobaiti, A. Althobaiti, R. I. Nuruddeen, H. S. Sambo, A. F. Aljohani, Solitonic analysis of the newly introduced three-dimensional nonlinear dynamical equations in fluid mediums, *Mathematics*, **12** (2024), 3205. https://doi.org/10.3390/math12203205
8. S. Althobaiti, A. M. Mubaraki, R. I. Nuruddeen, Dispersion of flexural waves on an initially pre-stressed thin plate resting on nonlinear elastic foundations, *Acta Mech.*, **236** (2025), 6141–6159. https://doi.org/10.1007/s00707-025-04458-8
9. M. M. A. Khater, Precision in wave propagation and bifurcation analysis: advanced symbolic techniques for nonlinear dynamics in fluid and plasma systems, *Nonlinear Dyn.*, **113** (2025), 20075–20095 . https://doi.org/10.1007/s11071-025-11140-0
10. A. K. H. Sedeeg, R. I. Nuruddeen, J. F. Gomez-Aguilar, Generalized optical soliton solutions to the (3+1)-dimensional resonant nonlinear Schrödinger equation with Kerr and parabolic law nonlinearities, *Opt. Quant. Electron.*, **51** (2019), 173. https://doi.org/10.1007/s11082-019-1889-6
11. M. Inc, A. I. Aliyu, A. Yusuf, D. Baleanu, Optical solitons to the resonance nonlinear Schrödinger equation by Sine-Gordon equation method, *Superlattices Micro.*, **113** (2018), 541–549. https://doi.org/10.1016/j.spmi.2017.11.035
12. K. K. Ahmed, N. M. Badra, H. M. Ahmed, W. B. Rabie, Unveiling optical solitons and other solutions for fourth-order (2+ 1)-dimensional nonlinear Schrödinger equation by modified

extended direct algebraic method, *J. Opt.*, **54** (2025), 2570–2582. https://doi.org/10.1007/s12596-024-01690-8

13. A. Biswas, Y. Yıldırım, E. Yaşar, Q. Zhou, A. S. Alshomrani, S. P. Moshokoa, et al., Solitons for perturbed Gerdjikov-Ivanov equation in optical fibers and PCF by extended Kudryashov's method, *Opt. Quant. Electron.*, **50**, (2018), 149. https://doi.org/10.1007/s11082-018-1417-0
14. H. I. Abdel-Gawad, C. Park, Interactions of pulses produced by two-mode resonant nonlinear Schrödinger equations, *Results Phys.*, **24** (2021), 104113. https://doi.org/10.1016/j.rinp.2021.104113
15. A. E. Rateb, H. M. Ahmed, A. Darwish, M. Ammar, W. B. Rabie, Analytical wave families and stability dynamics in a modified complex Ginzburg-Landau model via the modified extended direct algebraic method, *Sci. Rep.*, **16** (2026), 7485. https://doi.org/10.1038/s41598-026-37824-0
16. W. B. Rabie, H. B. Amer, H. Khan, J. Alzabut, D. l. Elimy, Exact solutions and stability thresholds for the fractional Gardner equation with high-order dispersion, *Eur. J. Pure Appl. Math.*, **19** (2026), 6805. https://doi.org/10.29020/nybg.ejpam.v19i1.6805
17. W. B. Rabie, H. M. Ahmed, M. Marin, M. F. Ismail, Exact wave solutions for rotational effects in temperature-dependent thermoelastic materials via IMETF technique, *Iran J. Sci. Technol. Trans. Mech. Eng.*, **50** (2026), 1–28. https://doi.org/10.1007/s40997-025-00917-8
18. I. Samir, H. M. Ahmed, W. Rabie, W. Abbas, O. Mostafa, Construction optical solitons of generalized nonlinear Schrodinger equation with quintuple power-law nonlinearity using Exp-function, projective Riccati, and new generalized methods, *AIMS Mathematics*, **10** (2025), 3392–3407. https://doi.org/10.3934/math.2025157
19. W. B. Rabie, H. M. Ahmed, M. S. Hashemi, M, Mirzazadeh, M. Bayram, Generating optical solitons in the extended (3+1)-dimensional nonlinear Kudryashov's equation using the extended F-expansion method, *Opt. Quant. Electron.*, **56** (2024), 894. https://doi.org/10.1007/s11082-024-06787-9
20. N. M. Kamel, H. M. Ahmed, W. B. Rabie, Retrieval of soliton solutions for 4th-order (2+1)-dimensional Schrödinger equation with higher-order odd and even terms by modified Sardar sub-equation method, *Ain Shams Eng. J.*, **15** (2024), 102808. https://doi.org/10.1016/j.asej.2024.102808
21. Y. Wang, W. R. Shan, X. Zhou, P. P. Wang, Exact solutions and bifurcation for the resonant nonlinear Schrödinger equation with competing weakly nonlocal nonlinearity and fractional temporal evolution, *Waves Random Complex Media*, **31** (2021), 1859–1878. https://doi.org/10.1080/17455030.2019.1706013
22. H. Triki, T. Hayat, O. M. Aldossary, A. Biswas, Bright and dark solitons for the resonant nonlinear Schrödinger equation with time-dependent coefficients, *Opt. Laser Technol.*, **44** (2012), 2223–2231. https://doi.org/10.1016/j.optlastec.2012.01.037
23. M. Mirzazadeh, M. Eslami, B. F. Vajargah, A. Biswas, Optical solitons and optical rogons of generalized resonant dispersive nonlinear Schrödinger's equation with power law nonlinearity, *Optik*, **125** (2014), 4246–4256. https://doi.org/10.1016/j.ijleo.2014.04.014
24. M. Ekici, Q. Zhou, A. Sonmezoglu, J. Manafian, M. Mirzazadeh, The analytical study of solitons to the nonlinear Schrödinger equation with resonant nonlinearity, *Optik*, **130** (2017), 378–382. https://doi.org/10.1016/j.ijleo.2016.10.098

25. K. K. Ahmed, N. M. Badra, H. M. Ahmed, W. B. Rabie, M. Mirzazadeh, M. Eslami, et al., Investigation of solitons in magneto-optic waveguides with Kudryashov's law nonlinear refractive index for coupled system of generalized nonlinear Schrödinger's equations using modified extended mapping method, *Nonlinear Anal.-Model.*, **29** (2024), 205–223. https://doi.org/10.15388/namc.2024.29.34070
26. I. Samir, A. H. Arnous, Y. Yildirim, A. L. Moraru, S. Moldovanu, Optical solitons with cubic-quintic-septic-nonic nonlinearities and quadrupled power-law nonlinearity: An observation, *Mathematics*, **10** (2022), 4085. https://doi.org/10.3390/math10214085
27. M. Eslami, M. Mirzazadeh, A. Biswas, Soliton solutions of the resonant nonlinear Schrödinger's equation in optical fibers with time dependent coefficients by simplest equation approach, *J. Mod. Opt.*, **60** (2013), 1627–1636. https://doi.org/10.1080/09500340.2013.850777
28. M. Mirzazadeh, M. Eslami, D. Milovic, A. Biswas, Topological solitons of resonant nonlinear Schödinger's equation with dual-power law nonlinearity by G'/G-expansion technique, *Optik*, **125** (2014), 5480–5489. https://doi.org/10.1016/j.ijleo.2014.03.042
29. S. A. AlQahtani, M. E. M. Alngar, Soliton solutions of perturbed NLSE-CQ model in polarization-preserving fibers with cubic-quintic-septic-nonic nonlinearities, *J. Opt.*, **53** (2024), 3789–3796. https://doi.org/10.1007/s12596-023-01526-x
30. S. Hussain, M. S. Iqbal, M. Bayram, R. Ashraf, M. Inc, S. Rezapour, et al., Optical soliton solutions in a distinctive class of nonlinear Schrödinger's equation with cubic, quintic, septic, and nonic nonlinearities, *Opt. Quant. Electron.* **56** (2024), 1066. https://doi.org/10.1007/s11082-024-06972-w
31. H. Ur Rehman, I. Iqbal, M. S. Hashemi, M. Mirzazadeh, M. Eslami, Analysis of cubic-quartic-nonlinear Schrödinger's equation with cubic-quintic-septic-nonic form of self-phase modulation through different techniques, *Optik*, **287** (2023), 171028. https://doi.org/10.1016/j.ijleo.2023.171028
32. D. Chen, Z. Li, Optical solitons of the cubic-quartic-nonlinear Schrödinger's equation having cubic-quintic-septic-nonic form of self-phase modulation. *Optik*, **277** (2023), 170687. https://doi.org/10.1016/j.ijleo.2023.170687
33. A. Das, B. Karmakar, A. Biswas, Y. Yildirim, A. A. Alghamdi, Chirped periodic waves and solitary waves for a generalized derivative resonant nonlinear Schrödinger equation with cubic-quintic nonlinearity, *Nonlinear Dyn.*, **111** (2023), 15347–15371. https://doi.org/10.1007/s11071-023-08640-2
34. L. de Broglie, La structure atomique de la matière et du rayonnement et la Mécanique ondulatoire, *C. R. Acad. Sci. Paris*, **184** (1927), 273–274.
35. A. Hyder, White noise theory and general improved Kudryashov method for stochastic nonlinear evolution equations with conformable derivatives, *Adv. Differ. Equ.*, **2020** (2020), 236. https://doi.org/10.1186/s13662-020-02698-7
36. S. Althobaiti, M. A. Hawwa, Flexural edge waves in a thick piezoelectric film resting on a Winkler foundation, *Crystal*, **12** (2022), 640. https://doi.org/10.3390/cryst12050640
37. S. Althobaiti, R. I. Nuruddeen, A. M. Mubaraki, Elastodynamics of a damped coated half-space under the influence of rotation, Pasternak foundation and generalized contact conditions, *J. Vib. Eng. Technol.*, **13**, (2025), 336. https://doi.org/10.1007/s42417-025-01916-4

38. H. Qawaqneh, J. Manafian, M. Alharthi, Y. Alrashedi, Stability analysis, modulation instability, and beta-time fractional exact soliton solutions to the Van der Waals equation, *Mathematics*, **12** (2024), 2257. https://doi.org/10.3390/math12142257
39. U. Demirbilek, A. H. Tedjani, A. R. Seadawy, Analytical solutions of the combined Kaitat II-X equation: A dynamical perspective on bifurcation, chaos, energy, and sensitivity, *AIMS Mathematics*, **10** (2025), 13664–13691. https://doi.org/10.3934/math.2025615
40. A. AlThemairi, R. I. Nuruddeen, R. B. Djob, Analytical solutions and analyses for the deflection of nonlinear waves on Kirchhoff plates underlying a Pasternak-like nonlinear elastic foundation, *Mathematics*, **14** (2026), 74. https://doi.org/10.3390/math14010074
41. Y. Chahlaoui, A. Ali, J. Ahmad, S. Javed, Dynamical behavior of chaos, bifurcation analysis and soliton solutions to a Konno-Onno model, *PLoS ONE*, **18** (2023), e0291197. https://doi.org/10.1371/journal.pone.0291197
42. N. A. Kudryashov, One method for finding exact solutions of nonlinear differential equations, *Commun. Nonlinear Sci.*, **17** (2012), 2248–2253. https://doi.org/10.1016/j.cnsns.2011.10.016
43. M. A. Salam, U. Habiba, Application of the improved Kudryashov method to solve the fractional nonlinear partial differential equations, *J. Appl. Math. Phys.*, **7** (2019), 912–920. https://doi.org/10.4236/jamp.2019.74061
44. F. Mahmuda, M. Samsuzzoha, M. A. Akbar, The generalized Kudryashov method to obtain exact traveling wave solutions of the PHI-four equation and the Fisher equation. *Results Phys.*, **7** (2017), 4296–4302. https://doi.org/10.1016/j.rinp.2017.10.049
45. S. Muhammad, A. Althobaiti, R. I. Nuruddeen, H. S. Sambo, H. Kim, Application of guaranteeing analytical methods in the construction of optical structures for nonlinear Schrodinger equations, *Modern Phys. Let. A*, **40** (2025), 2550189. https://doi.org/10.1142/S0217732325501895
46. E. M. E. Zayed, R. M. A. Shohib, M. E. M. Alngar, New extended generalized Kudryashov method for solving three nonlinear partial differential equations, *Nonlinear Anal. Model.*, **25** (2022), 598–617. https://doi.org/10.15388/namc.2020.25.17203
47. S. Althobaiti1, A. Althobaiti, Dynamic motion of a bifurcated beam supported by an array of nonlinear elastic springs: Solitonic and dispersion relation analyses, *AIP Adv.*, **15** (2025), 075117. https://doi.org/10.1063/5.0275430
48. Y. Yan, Y. F. Jiang, B. X. Li, C. S. Deng, Controlling dual fano resonance lineshapes based on an indirectly coupled double-nanobeam-cavity photonic molecule. *J. Lightwave Technol.*, **42** (2024), 732–739. https://doi.org/10.1109/JLT.2023.3318291
49. Z. X. Peng, B. X. Li, C. S. Deng, Ultrahigh-Q Fano resonance in a cavity-waveguide coupled system based on second-order topological photonic crystals with elliptical holes, *Opt. Laser Technol.*, **181** (2025), 111617. https://doi.org/10.1016/j.optlastec.2024.111617

AIMS Press